

Article

Effect of N-(2-Aminoethyl)-3-Aminopropyltrimethoxysilane on the Adhesion of the Modified Silicone Tie-Coating to Epoxy Primer

Hongyang Zhang, Yuhong Qi *, Zhanping Zhang and Qiang Yang

Department of Materials Science and Engineering, Dalian Maritime University, Dalian 116026, China; zhy686@dmlu.edu.cn (H.Z.); zzp@dmlu.edu.cn (Z.Z.); 1120180341yq@dmlu.edu.cn (Q.Y.)

* Correspondence: yuhong_qi@dmlu.edu.cn; Tel.: +86-411-8472-3556

Abstract: In this work, modified silicone tie-paints were prepared in a simple way for securing adhesion between the epoxy anticorrosive primer and silicone fouling release coating. Hydroxy-terminated polydimethylsiloxane (PDMS) mixture containing fillers and accessory ingredient was prepared as base component. N-(2-Aminoethyl)-3-aminopropyltrimethoxysilane (DAMO) was mechanically mixed with other functional additives as curing component. ATR-FTIR, XPS, SEM and tensile tests were used to investigate the chemical structure, morphology and mechanical properties of the tie-coatings. It was focused on the effect of the DAMO content on the adhesion of the tie-coating to epoxy primer. Peel off and shear tests were carried out to evaluate the adhesion. The results showed that introducing DAMO can significantly improve the properties of the tie-coating. The adhesion between the tie-coating and the epoxy primer increases with the increase of DAMO content, but the excessive DAMO content will decrease the fracture strength of the tie-coating and decrease the quality of the coating. When the DAMO content in tie-coating is 1.97 wt.%, the tie-coating performs excellent in the interlaminar adhesion, shear strength and mechanical properties.

Keywords: silicone tie-coating; epoxy primer; N-(2-Aminoethyl)-3-aminopropyltrimethoxysilane; adhesion



Citation: Zhang, H.; Qi, Y.; Zhang, Z.; Yang, Q. Effect of N-(2-Aminoethyl)-3-Aminopropyltrimethoxysilane on the Adhesion of the Modified Silicone Tie-Coating to Epoxy Primer. *Coatings* **2021**, *11*, 71. <https://doi.org/10.3390/coatings11010071>

Received: 20 November 2020

Accepted: 6 January 2021

Published: 9 January 2021

Publisher's Note: MDPI stays neutral with regard to jurisdictional claims in published maps and institutional affiliations.



Copyright: © 2021 by the authors. Licensee MDPI, Basel, Switzerland. This article is an open access article distributed under the terms and conditions of the Creative Commons Attribution (CC BY) license (<https://creativecommons.org/licenses/by/4.0/>).

1. Introduction

Human marine activities have long been plagued by biofouling. For example, biofouling on the surface of a ship will increase the weight of the ship, reduce its performance, corrosion promotion and increase the cost of hull maintenance [1,2]. Applying antifouling paints to the underwater structure of the ship is an effective way to solve biofouling. Traditional antifouling coatings (containing organic tin or cuprous oxide) are highly effective in controlling biofouling [3]. With the increasing importance of environmental protection to human beings, this type of antifouling coating has been banned [3]. Therefore, the nontoxicity of antifouling coatings is an inevitable trend of development [4].

Among non-toxic antifouling coatings, low surface energy antifouling coatings have become more and more popular. Low surface energy antifouling coatings rely on their own characteristics, making marine organisms only weakly adhere to the surface and readily removed by shear forces or other external forces [5,6]. Among the current low-surface antifouling coatings, silicone antifouling coating-based PDMS have been widely used due to the advantages of non-toxicity, low cost, an excellent antifouling effect and other advantages [7–10], but there are still some shortcomings involved in application [6]. For example, silicone antifouling coatings are often used in conjunction with epoxy primer due to epoxy primer having excellent mechanical, electrical, and bonding properties [11–14]. However, the interlaminar bonding strength between the silicone antifouling coatings and the epoxy primer were poor due to the surface properties of silicone such as low chemical reactivity and low surface energy [15–18].

In order to improve the interlaminar bonding strength between the silicone coating and the epoxy coating, researchers set about a technical approach at the levels of chemistry

and physics. On the one hand, Roth [16] et al. treated the rubber surface via low-pressure oxygen and ammonia plasma to form acidic or reactive surface groups which can form covalent bonds with epoxy groups of epoxy coating to enhance interlaminar bonding strength. However, the effect is instable and difficult to apply in engineering. Wang et al. [19] modified epoxy coating surface via corona discharge pretreatment, and the corona-pretreated surface was silanized with vinyltrimethoxysilane to generate vinyl groups, and finally reacted with the silicone resin to increase adhesion. However, this method requires special instruments, and the process was costly for engineering application. On the other hand, researchers incorporated epoxy resin into silicone resin by physical blending. However, the physical blending of silicone resin and epoxy resin would undoubtedly bring about incompatibility due to the huge difference in solubility parameter [18,20]. In order to improve this situation, silane coupling agents were introduced, and the functional groups of the silane coupling agents combine the two components [21–23]. In previous studies [9], various silane coupling agents were used as intermediates between epoxy coatings and silicone coatings to improve their compatibility. The only drawback was that the curing process was cumbersome. Xiong et al. [24] improved the adhesion properties of silicone coating by dispersing silanized epoxy resin into methyl phenyl silicone rubber and then cross-linking at room temperature. Zhou et al. [18] synthesized grafted copolymers containing a segment of siloxane on the side chain of an epoxy resin, and then the copolymer was dispersed into PDMS. This method significantly enhanced the adhesion performance of the silicone coatings. Inspired by this, we incorporated the silane coupling agent into PDMS through mechanical dispersion, and cured at room temperature to improve the adhesion properties of the silicone coating.

In this work, we designed a silicone tie-paint based on PDMS that was modified by N-(2-Aminoethyl)-3-aminopropyltrimethoxysilane (DAMO). The tie-paint is composed of binder and a functional agent component. The binder was made from PDMS, titanium dioxide, silicon dioxide, leveling agent, defoamer and dimethylbenzene, which were mixed and ground. Before painting, DAMO, tetraethyl orthosilicate (TEOS) and dibutyltin dilaurate (DBTDL) were mixed into the binder according to the formula ratio, the coating can be prepared. In this study, samples with varying DAMO contents in tie-coating were prepared, and the interfacial morphology, tensile properties, chemical structure of the tie-coating and interlaminar bonding strength between coatings were investigated. The aim of these works is to study the effect of DAMO on silicone tie-coating adhesion to epoxy primer.

2. Experimental

2.1. Materials

Epoxy primer Penguard HB was purchased from Jotun Coatings Co., Ltd. (Zhangjiakou, China). Silicone tie-paint was made by the laboratory, hydroxy-terminated polydimethylsiloxane (PDMS) was purchased from Dayi Chemical Co., Ltd. (Yantai, China), the kinematic viscosity of PDMS is 10,000 mm²/s. Silicon dioxide was purchased from Shenyang Chemical Co., Ltd. (Shenyang, China), the particle size was 5~40 nm. Titanium dioxide was purchased from Hongyunnyuan Chemical Co., Ltd. (Shanghai, China), the average particle size is 15 µm. N-(2-Aminoethyl)-3-aminopropyltrimethoxysilane (DAMO) was purchased from New Blue Sky New Materials Co., Ltd. (Wuhan, China). Tetraethyl orthosilicate (TEOS), dibutyltin dilaurate (DBTDL) and dimethylbenzene are all of analytical grade and purchased from Kemiou Chemical Reagent Co., Ltd. (Tianjin, China).

2.2. Preparation of the Specimen

Silicone tie-paint was composed by binder and functional agent component. The binder component was prepared by BGD 750 Versatile Sand-Milling Dispersing-agitator (Biuged Laboratory Instrument Supplies Co., Ltd., Guangzhou, China). The preparation process was as follows: PDMS was added to the BGD 750 Versatile Sand-Milling Dispersing-agitator, and silicon dioxide, titanium dioxide and accessory ingredient were slowly added at a speed of 1000 rpm, the speed was increased to 4000 rpm and blending for 30 min.

After blending was completed, it was ground by QZM conical mill (Precision Materials Instrument Testing Machine Factory, Tianjin, China) with discharge speed of 5 g/min, binder was stored in tinplate container after grinding. Before painting, mixed binder, DAMO, TEOS and DBTDL according to the formula ratio, finally adding an appropriate amount of solvent evenly, the coating can be prepared.

Samples were prepared according to the experimental design scheme. Samples were named TDX, in which X represents the tie-coating with X mass% of DAMO in the tie coating.

2.3. Characterizations

2.3.1. Microstructure and Morphology Analysis

Some tie-paint samples were spread onto 150 mm × 150 mm × 2 mm teflon mold, and demolded after curing 7 days in a high-low temperature damp heat test box at 25 °C and humidity of 60%, and then taken out for testing. The molecular structure of tie-coating was characterized by Frontier PerkinElmer infrared spectrometer (PerkinElmer Co., Ltd., Waltham, MA, USA) using the Attenuated Total Reflection (ATR) method. The scanning range was 4000–650 cm^{−1}. The resolution is 2 cm^{−1}. The number of scans was 32 times. Furthermore, tie-coating with air side and substrate side were also scanned by ESCALAB XI + X-ray photoelectron spectrometer (XPS) (Thermo Fisher, Waltham, MA, USA), the N elements were investigated. Each coating was tested three samples, and the results were analyzed.

In order to investigate the fracture morphology between two coatings, two coatings were prepared by air spraying to ensure that the same coatings were made with the same spraying pressure, speed, and spraying times. First, the epoxy primer was sprayed onto a 75 mm × 25 mm × 1 mm glass slide. Then the prepared tie-paint was sprayed on the surface of the epoxy primer after the surface drying. The epoxy primer or tie-coating in the sample was made from the same batch of paint to avoid errors in multiple measurements. Each layer of coating was completed, the coating thickness was measured by a film thickness meter and the most qualified sample was selected. Second, samples were allowed to cure for 7 days in a high-low temperature damp heat test box at 25 °C and humidity of 60%, taken out and deep-frozen in liquid nitrogen for 24 h, and knocked immediately, then taken out from liquid nitrogen. The fracture morphology of the sample was measured separately with the Carl Zeiss Supra 55 Scan Microscope (SEM) and the Olympus OLS4000 CLSM (OLYMPUS (China) Co., Ltd., Beijing, China). In order to ensure that the results are universal, we prepared three batches of samples in total, each batch of samples prepared under the same conditions. Six fractures were obtained for each sample for observation. The results were treated and the representative pictures are selected.

2.3.2. Tensile Tests

In order to investigate the tensile properties of the tie-coating, some tie-paint samples were prepared in a teflon mold with dimension of 150 mm × 150 mm × 2 mm. Samples were allowed to cure for 7 days in a high-low temperature damp heat test box at 25 °C and humidity of 60%, and then the cast film samples were taken out and cut into 45 mm × 4 mm dumbbell-shaped by dumbbell-shaped knife. According to national standard GB/T 528-2009 (ISO37-2005), samples were tested with the UTM 5105 computer-controlled electronic universal testing machine (Jinan Wance Electrical Equipment Co., Ltd., Jinan, China). The tensile speed is 50 mm/min. For each tie-coating, three reduplicate measurements were performed. The average of the elastic modulus, stress at 100%, fracture elongation and fracture strength were calculated and analyzed.

2.3.3. Crosslink Density

In order to investigate the crosslink density of the tie-coating, the crosslink density of the cast film sample was investigated by the equilibrium swelling method. The weighed cast film sample was put into a test tube containing 50 mL of methylbenzene, and it was immersed in a constant temperature water bath at 25 °C. The cast film sample was taken

out from methylbenzene every 3 h, the solvent on the surface was quickly absorbed with filter paper, and immediately put it into the weighing bottle was weighed with a precision electronic balance, and then the cast film sample was continuously swelled in the solvent until the difference between the two adjacent weighing results did not exceed 0.1 mg, the cast film sample is in a state of equilibrium swelling. The crosslink density of the cast film sample can be indicated by the relative molecular mass (M_c) between adjacent crosslinking points of the polymer. The relative molecular mass between adjacent cross-linking points of the sample was calculated according to the Flory-Rhener method. In order to ensure the accuracy of the data, each sample was tested six times, and the average value was taken to represent the M_c of the sample.

2.3.4. Interlaminar Shear Strength and Adhesion Test

Two coatings were prepared onto 150 mm × 70 mm × 1 mm steel plate which the preparation method of two coatings was the same as the glass slide sample. Samples were allowed to cure for 7 days in a high-low temperature damp heat test box at 25 °C and humidity of 60%, and taken out for testing. Cutting tool was used to cross-cut on the samples surface with the assistance of BGD 503 Cross Cutting Rule (Biuged Laboratory Instruments Co., Ltd., Guangzhou, China). The cutting interval was 1.5 mm, the distance between the grid area and the edge of the steel plate was not less than 5 mm, cut into a grid a grid of 100, then the PET silicone tape was glued to the grid area and peel off after 5 min at room temperature, observed and counted level of damage of each sample (Figure 1). The adhesion between tie-coating and epoxy primer was characterized according to the anti-peeling rate (APR), the APR of the sample was obtain according to the formula as following: $APR = \frac{100 - \text{number of peeled grid} - 0.25 \times \text{number of cocked edge}}{100} \times 100$.

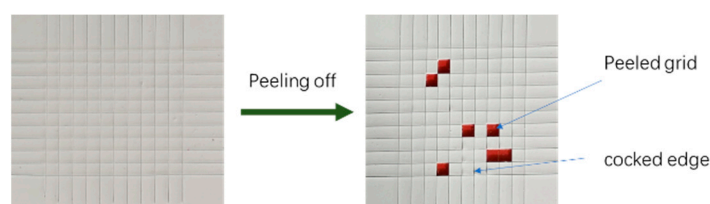


Figure 1. Schematic of interfacial strength evaluation.

The shear strength of the tie-coating/epoxy primer composite coatings was tested by the UTM5105 computer-controlled electronic universal testing machine (Jinan Wance Electrical Equipment Co., Ltd.) (Figure 2). The tensile speed was 20 mm/min. The sample preparation process was as follows: the two tinplate with dimension of 120 mm × 25 mm × 0.28 mm were overlapping placed in the same direction, and the overlapping area is 30 mm × 25 mm. Epoxy primer were coated separately to the inner surface of the overlapping area of the two tinplate by air spraying. The prepared tie-paint was sprayed onto the surface of the epoxy primer after the surface drying, and the two epoxy primer were tied through the tie-coating before surface drying. Samples were allowed to cure for 7 days in a high-low temperature damp heat test box at 25 °C and humidity of 60%, and then taken out for testing.

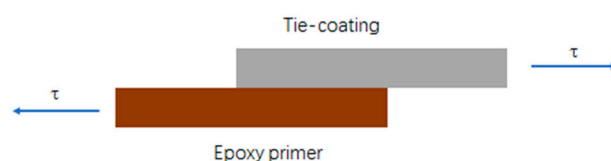


Figure 2. Schematic of shear test.

3. Results and Discussion

3.1. The Chemical Structure of the Silicone Tie-Coatings

3.1.1. ATR-FTIR

Figure 3 shows the infrared spectra of the tie-coating samples with varying DAMO contents. The absorption peak of the stretching vibration of the Si-Me₂ bond was at 788 cm⁻¹. The absorption peaks at 1008 cm⁻¹ and 1085 cm⁻¹ were attributed to the symmetric and anti-symmetric stretching vibration of the Si-O-Si bond. The absorption peak at 2963 cm⁻¹ was attributed to the anti-symmetric stretching vibration of the -CH₃ bond. The peaks between samples have no obvious difference. The intensity of absorption peak at the 3335 cm⁻¹ increased with increasing DAMO content. The absorption peak at 3335 cm⁻¹ was attributed to the N-H stretching vibration and -NH₂ anti-symmetric stretching vibration in DAMO, which illustrates the DAMO has been introduced into the tie-coating, which itself was realized by DAMO mechanically mixed into the binder.

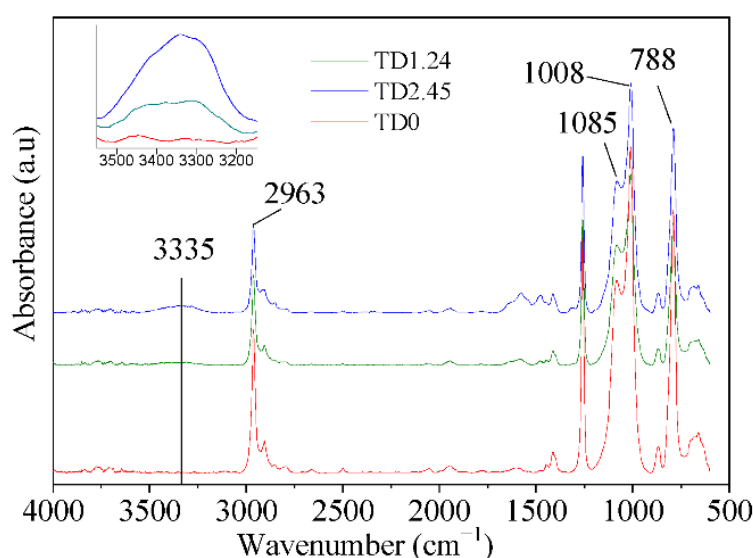


Figure 3. Infrared spectra of the typical silicone tie-coating samples. TD0 refers to the tie-coating sample without DAMO, TD1.24 refers to the tie-coating sample with DAMO of 1.24 wt.%, TD2.45 refers to the tie-coating sample with DAMO of 2.45 wt.%.

3.1.2. XPS

Figure 4a shows the X-ray photoelectron spectra (XPS) of the tie-coating samples. These analyses show the presence of Si, O, C elements in all the samples. N 1s scan spectra of all samples was shown in Figure 4b, and percentage of N atomic was also shown in Table 1. On the one hand, the intensity of the N 1s peak of each sample increased with the increasing DAMO content. In theory, TD0 does not contain N atomic, which may be caused by contamination of the sample surface. On the other hand, no matter the DAMO content being less or more in the coating, the intensity of the N 1s peak on the substrate side of each sample was higher than that of the air side. An inference can be drawn based on this phenomenon: the DAMO would migrate to the substrate side of the coating due to the priority curing of the surface of the coating. The DAMO content on the substrate side of the coating was more than that on the air side due to this phenomenon, and it was more conducive to more active hydrogen reacting with epoxy groups.

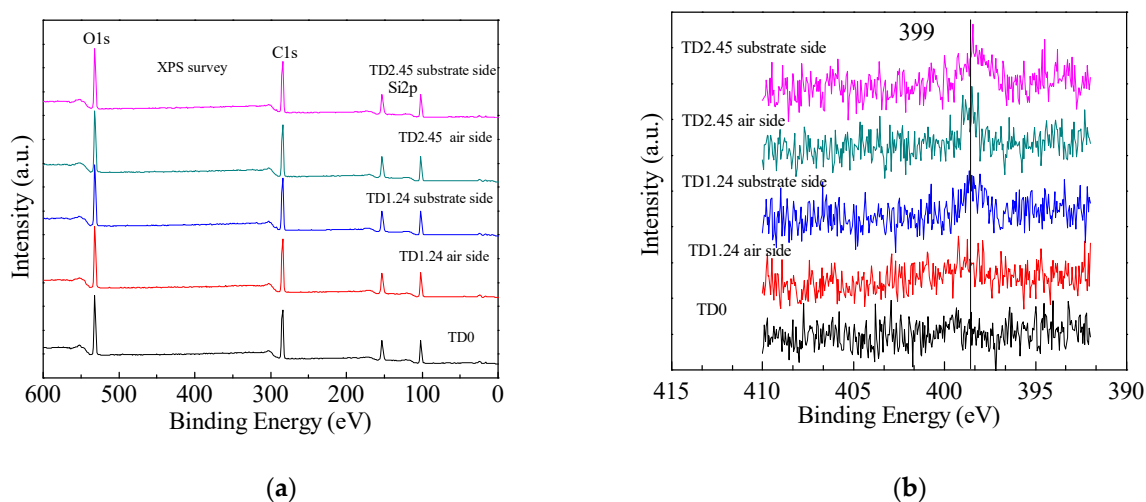


Figure 4. XPS analysis for typical samples: (a) XPS survey of samples; (b) N 1s scan of sample.

Table 1. Percentage of N Atomic.

Sample	TD0	TD1.24	TD2.45
Air side	–	0.36	0.68
Substrate side	0.06	0.47	0.79

3.2. The Tensile Properties of the Silicone Tie-Coatings

The tensile properties of the tie-coating samples were shown in Table 2, which shows that the tensile properties of the samples changed with the varies DAMO contents. Tensile curves of typical samples were shown in Figure 5. The results indicated that the elastic modulus, stress at 100%, fracture elongation and fracture strength of the sample without DAMO is lower than the sample with DAMO of 1.24 wt.%. When the DAMO content increases to 2.45 wt.%, those properties of the sample will decrease. This can be attributed to the crosslinking density changes with DAMO content increasing. The M_c value of the tie-coating samples were shown in the Table 3; the greater the M_c value, the lower the crosslink density of the coating. The crosslink density of TD0 is low due to insufficient TEOS content; a certain amount of DAMO was introduced into TD1.24 led to an increased crosslinking density compared with TD0. This can be attributed to the alkoxy group of DAMO being hydrolyzed in the presence of water, and then undergoing a dehydration condensation reaction with the hydroxyl groups at both ends of the PDMS, so the crosslink density of TD1.24 was increased. The content of DAMO continued to increase; the curing effect of DAMO was stronger than TEOS due to the high content of DAMO; DAMO played a leading role in the cross-linking process of the various molecular chains of PDMS, and the formation of a network structure with the silicon-oxygen chain was no existence due to the special structure of DAMO, so that the crosslink density of TD2.45 decreased. In addition, more DAMO would induce the number of PDMS molecular chains connecting with silicon dioxide to decrease [25]. The tensile properties of the tie-coating were changed due to these reasons.

Table 2. Tensile properties of typical tie-coating samples.

Sample	Elastic Modulus (MPa)	Stress at 100% (MPa)	Fracture Elongation (%)	Fracture Strength (MPa)
TD0	4.73 ± 0.01	0.38 ± 0.01	286.15 ± 2.87	0.81 ± 0.02
TD1.24	7.73 ± 0.15	0.47 ± 0.02	307.90 ± 4.03	0.87 ± 0.01
TD2.45	7.12 ± 0.20	0.41 ± 0.01	257.10 ± 5.34	0.66 ± 0.04

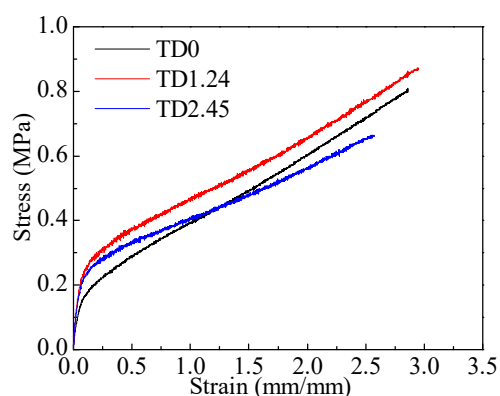


Figure 5. Tensile curves of typical silicone tie-coating samples.

Table 3. Mc value of typical tie-coating samples.

Sample	TD0	TD1.24	TD2.45
Mc	5965.50 ± 64.09	4495.98 ± 100.20	4916.34 ± 42.30

3.3. Interlaminar Adhesion and Shear Strength

Excellent connection property is very important for the tie-coating. The property could be indicated by anti-peeling rate (APR). The APR of the samples were shown in Figure 6. The result showed that the APR was significantly improved by adding a certain amount of DAMO. The sample with DAMO content of 1.97 wt.% and the APR of the tie-coating on the epoxy primer was 100%. This shows that DAMO content in the tie-coating was enough could improve adhesion between the tie-coating and epoxy primer.

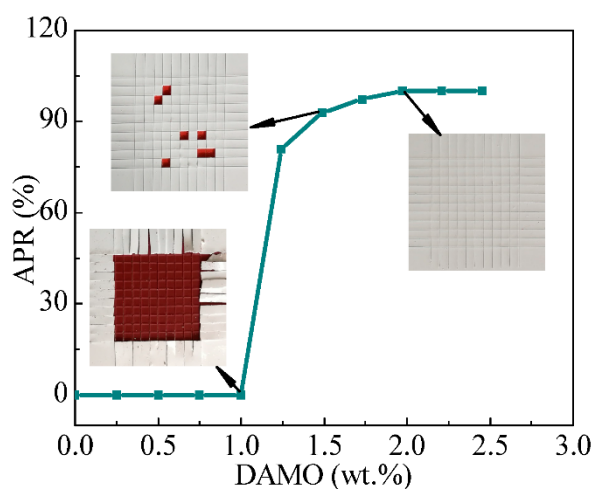


Figure 6. Effect of the DAMO content on the APR of the tie-coating on epoxy primer.

In the application of silicone antifouling coating, the attached organisms were removed when ships reached a certain speed. During this process, the coating was subjected to large shear force. In addition, the main destruction method of the coating was shear failure. Therefore, the shear strength of the tie coating/epoxy primer composite coatings was tested by a tensile testing machine. The result was shown in the Figure 7. The shear strength was influenced by DAMO content significantly, the shear strength of the sample without DAMO was lower than that of containing DAMO, and the shear strength at breaking increased as the DAMO content increased. The greatest value of shear strength at breaking was 0.29 MPa that obtained through the sample with DAMO content of 2.21 wt.%, the capability of damping external stresses was improved significantly. In addition, the fracture

position of the samples varied with the DAMO content. The tie-coating without DAMO was completely peeled off from the epoxy primer and the epoxy primer was completely exposed. With the increase of DAMO content in tie-coating, the fracture position changed from the interface of the epoxy primer to the inside of the tie-coating and the exposed area of the epoxy primer decreased.

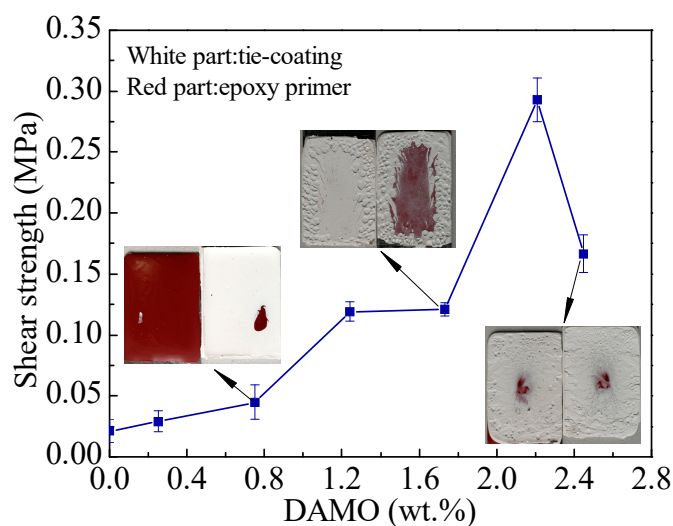


Figure 7. Effect of the DAMO content on shear strength of the tie coating/epoxy primer composite coatings.

3.4. Effect of the DAMO Content on Fracture Morphology of the Tie-Coating/Epox Primer Composite Coatings

In order to more intuitively study the connection behavior between the tie-coating and the epoxy primer, the tie-coating/epoxy primer composite coating sample was placed in liquid nitrogen, deep-frozen, and knocked off to obtain fracture. The fracture morphology of samples with varying DAMO contents was investigated by CLSM and results are shown in Figure 8. The DAMO content would affect the fracture morphology. There is a gap between the tie-coating without DAMO and epoxy primer (Figure 8a), this indicates the adhesion between coatings is very poor. In Figure 8b, the fracture morphology of the sample with DAMO content of 1.24 wt.% in tie-coating was a step profile. This phenomenon can be explained as follows: The interface bonding strength of the two coatings in TD1.24 was different in different areas due to insufficient DAMO content. Under the action of external force, coating would bend out of shape, the two coatings would not separate in the area with high interface bonding strength, and the two coatings would occur separate in the area with poor interface bonding strength, breaking occur when the deformation exceeds the breaking limit of the material. During the deformation process, the separation of the two coatings starts from the area with poor interface bonding strength and ends at the area with high interface bonding strength. Differing from the overall poor interface bonding strength of the two coatings in TD0, the interface bonding strength of the two coatings in TD1.24 differs in different areas. If the breaking occurs in the area with poor interface bonding strength, the breaking process of the coatings will be influenced by the distribution characteristics of the area, which would cause the difference in the breaking position of the two coatings. In Figure 8c, when the content of DAMO in the tie-coating increased to 2.45 wt.%, the fracture morphology of the two coatings is relatively flat, and the interface bonding condition is good. This is attributed to the content of DAMO in tie-coating being increased, which improves the interface bonding strength with epoxy primer. When the external force was applied, the two coatings broke as a whole.

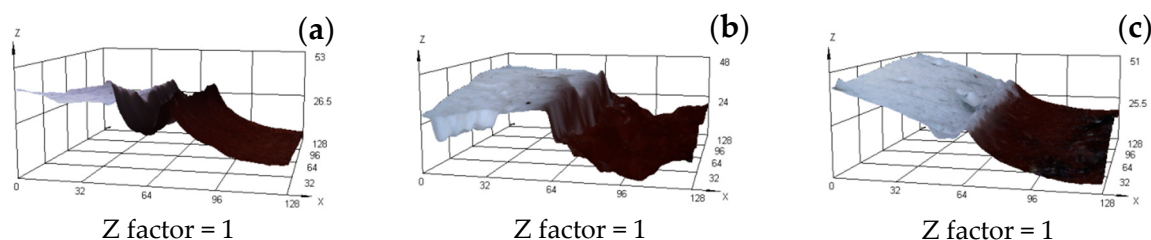


Figure 8. CLSM 3D images of typical fracture morphology: (a) TD0; (b) TD1.24; (c) TD2.45. The white part is tie-coating, the adjacent coating is epoxy primer.

To reveal more clearly the interlaminar bond structure, above-mentioned samples were observed by SEM. Their fractures were shown in Figure 9. It can be obviously found that the fracture morphology of between coatings was influenced by DAMO content. Figure 9a shows that there is an obvious gap between the tie-coating with DAMO content of 0 wt.% and epoxy primer, which indicates that the adhesion between the tie-coating without DAMO and epoxy primer is poor. In Figure 9b, the interface bonding quality was improved between the tie-coating with DAMO content of 1.24 wt.% and the epoxy primer, and there are still defects in some areas between coatings, which leads to poor local adhesion between the tie-coating and the epoxy primer, which was caused by insufficient DAMO content. In Figure 9c, with the increase of DAMO content in the tie-coating to 2.45 wt.%, the interface bonding condition between the tie-coating and epoxy primer is good, so TD2.45 showed excellent performance in the interlaminar adhesion. The effect of the DAMO content measured by SEM was consistent with the CLSM measurement result.

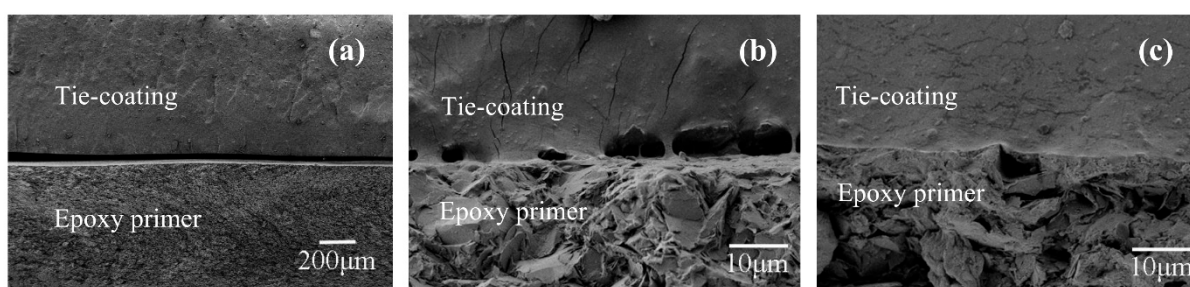


Figure 9. SEM image of typical fracture morphology: (a) TD0; (b) TD1.24; (c) TD2.45.

All the results show that DAMO modified tie-coating can improve the interlaminar bonding between the silicone coating and epoxy primer. The DAMO content in the tie-coating determines the interface bonding quality between coatings. The DAMO content was less, and so it was difficult to disperse the DAMO uniformly and the DAMO content per unit volume was also less. During film formation, the amount of DAMO on the surface of epoxy primer was less, and a little amount of epoxy groups was reacted (Figure 10a). Hence, the interlaminar adhesion was weak between coatings. With the increase of DAMO content, the interlaminar adhesion and shear strength was improved. The reason for the improvement was that only one active hydrogen was needed for the ring-opening reaction of an epoxy group form strong interaction, and the excess DAMO made epoxy groups participate in the reaction as much as possible [26]. From the results of infrared and XPS tests, it can be seen that the amount of active hydrogen involved in the reaction with epoxy groups in the tie-coating increased with the increase of DAMO content. In addition, the DAMO content affected the mechanical properties of the coating. We improved the adhesion between the tie-coating and the epoxy primer by increasing the DAMO content, but this also reduced the fracture strength of the tie-coating. The failure location of the coating adhesion transferred to the inside of the coating, which is also undesirable (Figure 10b).

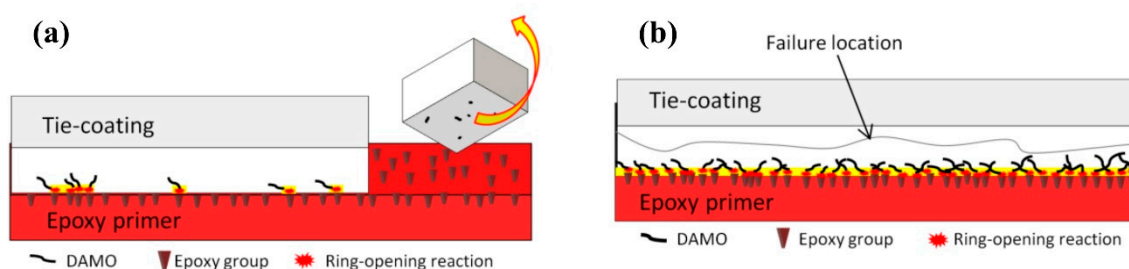


Figure 10. Schematic diagram of tie-coating failure: (a) interlaminar failure; (b) tie-coating fracture failure.

3.5. Tie Mechanism of the Silicone Tie-Coating Adhesion to Epoxy Primer

The tie-paint was prepared according to the formula ratio and then brushed on the epoxy primer. In the initial state, the solvent in the coating was not evaporated a lot, the coating had good fluidity, and the molecules diffused within the liquid coating that has not been cured. As the solvent in the coating evaporated in a large amount, the water in the air entered the coating. In the stage, the dealcoholized condensation reaction between ethoxy group of DAMO, TEOS and hydroxyl groups of PDMS took place in the presence of catalyst. On the surface of the epoxy primer, the active hydrogen in DAMO reacted with the unreacted epoxy group on the surface of epoxy primer, and the tie-coating was bonded to the epoxy primer by forming a chemical bond (Figure 11).

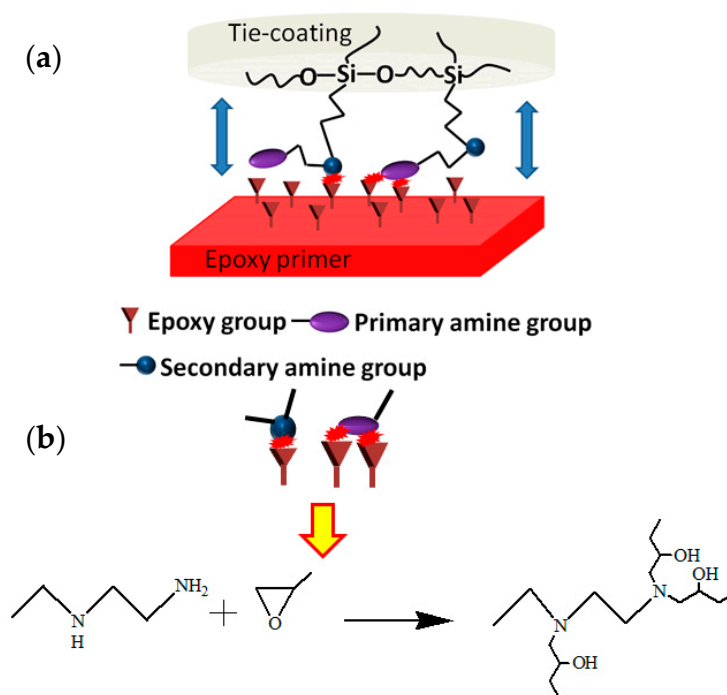


Figure 11. The tie method between epoxy primer and silicone tie-coating: (a) Schematic diagram of tie mechanism; (b) reaction formula.

4. Conclusions

In the present study, DAMO modified silicone tie-coatings were prepared to improve the adhesion with epoxy primers. This preparation method is simple and easy to implement. The effect of the DAMO content on the adhesion between the tie-coating and epoxy primer was investigated. Results show that the DAMO content in the tie-coating exceeded 1 wt.% and the adhesion between the tie-coating and the epoxy primer was significantly improved compared to the tie-coating without DAMO. However, the amount of DAMO was over

1.97 wt.%, which will result in a decrease in the fracture strength of coating and a decrease in the quality of the coating. Therefore, the appropriate DAMO content is very important to the overall performance of the coating. Through verifications, the tie-coating with DAMO content of 1.97 wt.% performed excellent in the interlaminar adhesion, shear strength and mechanical properties.

Author Contributions: Conceptualization, H.Z., Y.Q., and Z.Z.; methodology, H.Z., Y.Q., and Z.Z.; validation, H.Z. and Z.Z.; formal analysis, H.Z., Y.Q., and Z.Z.; investigation, H.Z. and Q.Y.; resources, Y.Q. and Z.Z.; data curation, H.Z. and Q.Y.; writing—original draft preparation, H.Z. and Y.Q.; writing—review and editing, H.Z., Z.Z., and Y.Q.; visualization, H.Z.; supervision, Z.Z. and Y.Q.; project administration, Z.Z. and Y.Q.; funding acquisition, Z.Z. and Y.Q. All authors have read and agreed to the published version of the manuscript.

Funding: This research is supported by the National Science Foundation of China (51,879,021), Project of Equipment Pre-research Field Fund (61,409,220,304) and Equipment Pre-research Sharing Technology Project (41,404,010,306 and 41,423,060,314).

Institutional Review Board Statement: Not applicable.

Informed Consent Statement: Not applicable.

Data Availability Statement: Data is contained within the article.

Conflicts of Interest: The authors declare no conflict of interest.

References

1. Xie, Q.Y.; Pan, J.S.; Ma, C.F.; Zhang, G.Z. Dynamic surface antifouling: Mechanism and systems. *Soft Matter* **2019**, *15*, 1087–1107. [[CrossRef](#)] [[PubMed](#)]
2. Liu, C.; Ma, C.; Xie, Q.; Zhang, G. Self-repairing silicone coating for marine antifouling-biofouling. *J. Mater. Chem. A* **2017**, *5*, 15855–15861. [[CrossRef](#)]
3. Leonardi, A.K.; Ober, C.K. Polymer-Based Marine Antifouling and Fouling Release Surfaces: Strategies for Synthesis and Modification. *Annu. Rev. Chem. Biomol. Eng.* **2019**, *10*, 241–264. [[CrossRef](#)] [[PubMed](#)]
4. Ouyang, Y.; Zhao, J.; Qiu, R.; Hu, S.G.; Zhang, Y.; Wang, P. Bioinspired superhydrophobic and oil-infused surface: Which is the better choice to prevent marine biofouling? *Colloids Surf. A Physicochem. Eng. Aspects* **2018**, *559*, 297–304. [[CrossRef](#)]
5. Yang, M.S.; Sun, Y.H.; Chen, G.M.; Wang, G.Y.; Lin, S.Z.; Sun, Z.Y. Preparation of a self-healing silicone coating for inhibiting adhesion of benthic diatoms. *Mater. Lett.* **2020**, *268*, 127496. [[CrossRef](#)]
6. Hu, P.; Xie, Q.Y.; Ma, C.F. Fouling resistant silicone coating with self-healing induced by metal coordination. *Chem. Eng. J.* **2021**, *406*, 126870. [[CrossRef](#)]
7. Mirabedini, S.M.; Pazoki, S.; Esfandeh, M.; Mohseni, M.; Akbari, Z. Comparison of drag characteristics of self-polishing copolymers and silicone foul release coatings: A study of wettability and surface roughness. *Prog. Org. Coat.* **2006**, *57*, 421–429. [[CrossRef](#)]
8. Zhang, Y.; Qi, Y.H.; Zhang, Z.P. Synthesis of PPG-TDI-BDO polyurethane and the influence of hard segment content on its structure and antifouling properties. *Prog. Org. Coat.* **2016**, *97*, 115–121. [[CrossRef](#)]
9. Esfandeh, M.; Mirabedini, S.M.; Pazokifard, S.; Tari, M. Study of silicone coating adhesion to an epoxy undercoat using silane compounds: Effect of silane type and application method. *Colloids Surf. A Physicochem. Eng. Asp.* **2007**, *302*, 11–16. [[CrossRef](#)]
10. Selim, M.S.; Shenashen, M.A.; El-Safty, S.A.; Higazy, S.A.; Selim, M.M.; Isago, H.; Elmarakbi, A. Recent progress in marine foul-release polymeric nanocomposite coatings. *Prog. Mater. Sci.* **2017**, *87*, 1–32. [[CrossRef](#)]
11. Khurana, P.; Aggarwal, S.; Narula, A.K.; Choudhary, V. Studies on curing and thermal behaviour of DGEBA in the presence of bis (4-carboxyphenyl) dimethyl silane. *Polym. Int.* **2003**, *52*, 908–917. [[CrossRef](#)]
12. Ochi, M.; Shimaoka, S. Phase structure and toughness of silicone-modified epoxy resin with added silicone graft copolymer. *Polymer* **1999**, *40*, 1305–1312. [[CrossRef](#)]
13. Lee, S.S.; Kim, S.C. Morphology and properties of polydimethylsiloxane- modified epoxy resin. *J. Appl. Polym. Sci.* **1997**, *64*, 941–955. [[CrossRef](#)]
14. Ahmad, S.; Gupta, A.P.; Sharmin, E.; Alam, M.; Pandey, S.K. Synthesis, characterization and development of high performance siloxane-modified epoxy paints. *Prog. Org. Coat.* **2005**, *54*, 248–255. [[CrossRef](#)]
15. Svendsen, J.R.; Kontogeorgis, G.M.; Kiil, S.; Weinell, C.E.; Grønlund, M. Adhesion between coating layers based on epoxy and silicone. *J. Colloid Interface Sci.* **2007**, *316*, 678–686. [[CrossRef](#)]
16. Roth, J.; Albrecht, V.; Nitschke, M.; Bellmann, C.; Simon, F.; Zschoche, S.; Michel, S.; Luhmann, C.; Grundke, K.; Voit, B. Surface functionalization of silicone rubber for permanent adhesion improvement. *Langmuir* **2008**, *24*, 12603–12611. [[CrossRef](#)]
17. Eddington, D.T.; Puccinelli, J.P.; Beebe, D.J. Thermal aging and reduced hydrophobic recovery of polydimethylsiloxane. *Sens. Actuators B Chem.* **2006**, *114*, 170–172. [[CrossRef](#)]

18. Zhou, C.; Li, R.; Luo, W.; Chen, Y.; Zou, H.W.; Liang, M.; Li, Y. The preparation and properties study of polydimethylsiloxane-based coatings modified by epoxy resin. *J. Polym. Res.* **2016**, *23*, 14. [[CrossRef](#)]
19. Wang, F.; Li, Y.; Wang, D. Adhesion enhancement for liquid silicone rubber and different surface by organosilane and Pt catalyst at room temperature. *Bull. Mater. Sci.* **2013**, *36*, 1013–1017. [[CrossRef](#)]
20. Rath, S.K.; Chavan, J.G.; Sasane, S.; Jagannath; Patri, M.; Samui, A.B.; Chakraborty, B.C. Two component silicone modified epoxy fowl release coatings: Effect of modulus, surface energy and surface restructuring on pseudobarnacle and macrofouling behavior. *Appl. Surf. Sci.* **2010**, *256*, 2440–2446. [[CrossRef](#)]
21. Vreugdenhil, A.J.; Gelling, V.J.; Woods, M.E.; Schmelz, J.R.; Enderson, B.P. The role of crosslinkers in epoxy–amine crosslinked silicon sol–gel barrier protection coatings. *Thin Solid Film.* **2008**, *517*, 538–543. [[CrossRef](#)]
22. Suleiman, R.; Dafalla, H.; El Ali, B. Novel hybrid epoxy silicone materials as efficient anticorrosive coatings for mild steel. *RSC Adv.* **2015**, *5*, 39155–39167. [[CrossRef](#)]
23. Harblin, O.M. Method of Modifying Epoxy-Coated Ship's Hull Surfaces, and Surfaces Obtained Thereby. U.S. Patent No. 6,110,536, 29 August 2000.
24. Xiong, G.; Kang, P.; Zhang, J.C.; Li, B.W.; Yang, J.Y.; Chen, G.X.; Zhou, Z.; Li, Q.F. Improved adhesion, heat resistance, anticorrosion properties of epoxy resins/POSS/methyl phenyl silicone coatings. *Prog. Org. Coat.* **2019**, *135*, 454–464. [[CrossRef](#)]
25. Su, X.; Shi, B. Effect of silane coupling agents with different non-hydrolytic groups on tensile modulus of composite PDMS crosslinked membranes. *React. Funct. Polym.* **2016**, *98*, 1–8. [[CrossRef](#)]
26. Gong, X.Y.; Liu, Y.Y.; Wang, Y.S.; Xie, Z.M.; Dong, Q.L.; Dong, M.Y.; Liu, H.; Shao, Q.; Lu, N.; Murugadoss, V.; et al. Amino graphene oxide/dopamine modified aramid fibers: Preparation, epoxy nanocomposites and property analysis. *Polymer* **2019**, *168*, 131–137. [[CrossRef](#)]